

<https://helda.helsinki.fi>

Insulin-inducible THRSP maintains mitochondrial function and regulates sphingolipid metabolism in human adipocytes

Ahonen, Maria A.

2022-12

Ahonen , M A , Höring , M , Nguyen , V D , Qadri , S , Taskinen , J H , Nagaraj , M , Wabitsch , M , Fischer-Posovszky , P , Zhou , Y , Liebisch , G , Haridas , P A N , Yki-Järvinen , H & Olkkonen , V M 2022 , ' Insulin-inducible THRSP maintains mitochondrial function and regulates sphingolipid metabolism in human adipocytes ' , Molecular Medicine , vol. 28 , no. 1 , 68 . <https://doi.org/10.1186/s10020-022-00496-3>

<http://hdl.handle.net/10138/346350>

<https://doi.org/10.1186/s10020-022-00496-3>

cc_by

publishedVersion

Downloaded from Helda, University of Helsinki institutional repository.

This is an electronic reprint of the original article.

This reprint may differ from the original in pagination and typographic detail.

Please cite the original version.

RESEARCH ARTICLE

Open Access



Insulin-inducible THRSP maintains mitochondrial function and regulates sphingolipid metabolism in human adipocytes

Maria A. Ahonen^{1,2}, Marcus Höring³, Van Dien Nguyen⁴, Sami Qadri^{1,6}, Juuso H. Taskinen¹, Meghana Nagaraj¹, Martin Wabitsch⁵, Pamela Fischer-Posovszky⁴, You Zhou⁵, Gerhard Liebisch³, P. A. Nidhina Haridas¹, Hannele Yki-Järvinen^{1,6} and Vesa M. Olkkonen^{1,7*}

Abstract

Background: Thyroid hormone responsive protein (THRSP) is a lipogenic nuclear protein that is highly expressed in murine adipose tissue, but its role in humans remains unknown.

Methods: We characterized the insulin regulation of THRSP in vivo in human adipose tissue biopsies and in vitro in Simpson-Golabi-Behmel syndrome (SGBS) adipocytes. To this end, we measured whole-body insulin sensitivity using the euglycemic insulin clamp technique in 36 subjects [age 40 ± 9 years, body mass index (BMI) 27.3 ± 5.0 kg/m²]. Adipose tissue biopsies were obtained at baseline and after 180 and 360 min of euglycemic hyperinsulinemia for measurement of *THRSP* mRNA concentrations. To identify functions affected by THRSP, we performed a transcriptomic analysis of THRSP-silenced SGBS adipocytes. Mitochondrial function was assessed by measuring mitochondrial respiration as well as oxidation and uptake of radiolabeled oleate and glucose. Lipid composition in THRSP silencing was studied by lipidomic analysis.

Results: We found insulin to increase *THRSP* mRNA expression 5- and 8-fold after 180 and 360 min of in vivo euglycemic hyperinsulinemia. This induction was impaired in insulin-resistant subjects, and *THRSP* expression was closely correlated with whole-body insulin sensitivity. In vitro, insulin increased both *THRSP* mRNA and protein concentrations in SGBS adipocytes in a phosphoinositide 3-kinase (PI3K)-dependent manner. A transcriptomic analysis of THRSP-silenced adipocytes showed alterations in mitochondrial functions and pathways of lipid metabolism, which were corroborated by significantly impaired mitochondrial respiration and fatty acid oxidation. A lipidomic analysis revealed decreased hexosylceramide concentrations, supported by the transcript concentrations of enzymes regulating sphingolipid metabolism.

Conclusions: THRSP is regulated by insulin both in vivo in human adipose tissue and in vitro in adipocytes, and its expression is downregulated by insulin resistance. As THRSP silencing decreases mitochondrial respiration and fatty acid oxidation, its downregulation in human adipose tissue could contribute to mitochondrial dysfunction. Furthermore, disturbed sphingolipid metabolism could add to metabolic dysfunction in obese adipose tissue.

Keywords: Hexosylceramide, Insulin sensitivity, Oxidation, Thyroid hormone

*Correspondence: vesa.olkkonen@helsinki.fi

¹ Minerva Foundation Institute for Medical Research, Biomedicum 2U, Tukholmankatu 8, 00290 Helsinki, Finland
Full list of author information is available at the end of the article

Introduction

The thyroid hormone sensitive protein (THRSP; Spot14; S14) is a nuclear protein, which is abundantly expressed in lipogenic tissues such as in liver, mammary gland, and



© The Author(s) 2022. **Open Access** This article is licensed under a Creative Commons Attribution 4.0 International License, which permits use, sharing, adaptation, distribution and reproduction in any medium or format, as long as you give appropriate credit to the original author(s) and the source, provide a link to the Creative Commons licence, and indicate if changes were made. The images or other third party material in this article are included in the article's Creative Commons licence, unless indicated otherwise in a credit line to the material. If material is not included in the article's Creative Commons licence and your intended use is not permitted by statutory regulation or exceeds the permitted use, you will need to obtain permission directly from the copyright holder. To view a copy of this licence, visit <http://creativecommons.org/licenses/by/4.0/>.

adipose tissue (AT) and lipogenic breast cancers (Freake and Moon 2003; Freake and Oppenheimer 1987; Jump 1989; Jump et al. 1984). In the rat liver, expression of THRSP is significantly induced by thyroid hormone stimulation (Jump 1989). Although THRSP was first characterized in 1981, data regarding its physiological functions remain inconclusive (Seelig et al. 1981). Zhu et al. showed that THRSP deletion in mice enhanced hepatic de novo lipogenesis, while Wu et al. reported a decrease in hepatic lipogenesis (Wu et al. 2013; Zhu et al. 2001). In whole-body knock-out mice, Anderson et al. reported a weight reduction, improved glucose tolerance, and enhanced insulin sensitivity, while several contradictory studies in animal models suggested a positive correlation between THRSP expression and insulin sensitivity, glucose tolerance, and lipid synthesis (Anderson et al. 2009; Cao et al. 2007; Wang et al. 2007, 2004).

Data are sparse regarding the role of THRSP in human metabolism. Serum and AT levels of the protein are decreased in subjects with the metabolic syndrome, while its expression is upregulated during adipogenic differentiation (Chen et al. 2019; Ortega et al. 2010). These findings suggest a functional role for THRSP in healthy AT expansion. Importantly, our group has previously found THRSP to be one of the top-regulated genes in micro array analysis of human AT upon infusion with insulin (Soronen et al. 2012). Whether THRSP acts as a mediator of insulin-regulated metabolic pathways in AT is unknown. In addition to lipid storage capacity, the composition of stored lipids affects adipocyte metabolism and signaling to other cell types (Ahonen et al. 2021; Leiria and Tseng 2020). There are, however, no studies showing whether THRSP modulates adipocyte lipid composition.

Mitochondrial dysfunction has a detrimental impact on adipocyte metabolism and is thought to contribute to the pathogenesis of obesity, insulin resistance, and type 2 diabetes (Lowell and Shulman 2005; Rocha et al. 2020; Van Der Kolk et al. 2021). Thyroid hormones impact the mitochondrial function by alterations of ATP synthesis, oxidative phosphorylation, fatty acid transport and mitochondria biogenesis (Harper and Seifert 2008; Sinha et al. 2018; Weitzel et al. 2003). However, the role of THRSP in mediating the mitochondrial effects of thyroid hormones is unclear.

As we hypothesized THRSP to be a likely regulator of adipocyte metabolism, we systematically assessed its functions in human AT in vivo and in a cultured human adipocyte model in vitro. Specifically, we wished to validate the induction of THRSP by insulin in human adipocytes and to determine whether THRSP is a potential mediator of lipogenic actions of insulin in humans. To this end, we studied *THRSP* expression in AT biopsies

of 36 individuals, obtained during euglycemic hyperinsulinemia. We further replicated the analysis in cultured adipocytes and determined whether silencing of THRSP conferred transcriptional changes in central metabolic pathways. As this was found to be the case, we studied the effects of THRSP silencing on cellular mitochondrial functions and on the adipocyte lipidome.

Materials and methods

Subjects and design of the clinical study

We recruited a total of 36 non-diabetic volunteers based on the following inclusion criteria: (a) age 18–60 years; (b) a body mass index (BMI) ≤ 40 kg/m²; (c) no evidence of acute or chronic disease other than obesity based on history, physical examination, electrocardiogram, and standard laboratory tests (complete blood counts, serum creatinine, thyrotropin, and electrolyte concentrations); (d) no use of drugs potentially affecting glucose tolerance; and (e) not pregnant or lactating. All volunteers were women. Each subject underwent a history and physical examination, including measurement of body weight and height. Fasting blood samples were drawn for measurement of plasma glucose, serum insulin, and serum C-peptide concentrations. The percentage of body fat was determined by using a bioelectrical impedance analysis (BioElectrical Impedance Analyzer System Model #BIA-101A; RJL Systems, Detroit, MI, USA). Subcutaneous fat volume was determined using magnetic resonance imaging, as previously described in detail (Ryysy et al. 2000). Whole-body insulin sensitivity of each subject was determined using the euglycemic hyperinsulinemic clamp technique (DeFronzo et al. 1979; Westerbacka et al. 2006; Yki-Jarvinen et al. 1984). Briefly, we used a primed-continuous infusion of regular human insulin (Insulin Actrapid; Novo Nordisk, Denmark), with the continuous part of infusion given at a rate of 1 mU/kg·min for 6 h. Normoglycemia was maintained by adjusting the rate of a 20% glucose infusion, based on plasma glucose measurements sampled every 5 min from arterialized venous blood. Aspiration needle biopsies of subcutaneous AT (SAT) were obtained before hyperinsulinemia and at 180 and 360 min after the start of the infusion. The biopsies were immediately snap-frozen in liquid nitrogen and subsequently stored at -80 °C until further analysis. Insulin sensitivity (M-value) of the subjects was calculated from the glucose infusion rate required to maintain normoglycemia from 30 to 360 min, and the median M-value was used to divide the subjects into insulin-sensitive (IS) and insulin-resistant (IR) groups (DeFronzo et al. 1979). Each participant provided a written informed consent after being explained the nature and potential risks of the study, which received approval from the Ethics

Committee of the Hospital District of Helsinki and Uusimaa (Helsinki, Finland).

Cell culture and transfections

We studied the function of THRSP by silencing or over-expressing the gene in human adipocytes. To silence THRSP, Simpson-Golabi-Behmel syndrome (SGBS) adipocytes were cultured and differentiated for 14 days (Fischer-Posovszky et al. 2008; Wabitsch et al. 2001). Mature adipocytes were then transfected with either 200 nM of THRSP siRNA (siRTHRSP; Ambion; AM16704, ID:12758) or Silencer Select™ non-targeting control 2 (SS2; Thermo Fisher Scientific 4390846, Waltham, MA), by using the RNAiMax™ transfection reagent (Thermo Fisher Scientific; 13778-150). Transfection complexes underwent incubation on the cells for 72 h, followed by lysing or further use for downstream experiments. Insulin induction of SGBS was performed by first starving the cells in serum-free low-glucose medium, and then treating with 100 nM insulin or insulin and 50 μM LY294002 (LY) overnight.

To overexpress THRSP in SGBS cells, the cells were cultured as specified above. Preadipocytes were then infected with lentiviral particles expressing THRSP (THRSP oex; accession number BC031989) or control particles generated from an empty pENTR2B vector (oex ctrl), along with polybrene (8 μg/ml). Transduction was carried out for 24 h, followed by switching to a serum-free medium. After 24 h, the medium was again replaced with a culture medium containing serum and blasticidin (20 μg/ml; Invitrogen; R210-01) for 2 days. Next, the cells were cultured and differentiated as specified above. The constructs were generated by the Genome Biology Unit, which is supported by HiLIFE and the Faculty of Medicine, University of Helsinki, and Biocenter Finland.

To further validate our observations made in human adipocytes, we repeated the key experiments in 3T3-L1 mouse adipocytes. The cells were differentiated as described previously (Mysore et al. 2017). Insulin induction was performed as specified above.

RNA sequencing

After the transfection of mature SGBS adipocytes with either siRTHRSP or SS2 (see above), the cells were lysed and their RNA extracted using the RNeasy mini kit (Qiagen; 74104), followed by DNase I treatment, according to the manufacturer's protocol. The library was prepared using the TruSeq Stranded mRNA kit (Illumina) according to manufacturer's protocol. Sequencing was performed on the Illumina NovaSeq 6000 platform using 2 × 100 bp paired-end reads for analysis. Demultiplexing of the sequencing reads was performed with Illumina bcl2fastq version 2.20. Adapters were trimmed

with Skewer version 0.2.2 (Jiang et al. 2014). The quality of FASTQ files was analyzed with FastQC version 0.11.5-cegat (Andrews 2010).

RNA-sequencing analysis was performed using the Chipster suite (Kallio et al. 2011) according to the following workflow: (1) FASTQ reads were trimmed using Trimmomatic (Bolger et al. 2014); (2) Trimmed pair-ended reads were aligned to the Homo sapiens GRCh38.95 genome using STAR (Dobin et al. 2013); (3) Aligned reads were counted using HTSeq (Anders et al. 2015); (4) Differential expression analysis was performed using DESeq2 (Love et al. 2014); (5) Ensembl identifiers were annotated using BioMaRt (Durinck et al. 2009).

For the Reactome pathway analysis, the list of differentially expressed genes (DEGs) was first filtered by Entrez names. Of duplicate Entrez IDs, the most significantly differentially expressed ones were used for downstream analysis. Subsequently, the Reactome pathway database was employed for the interrogation using the ReactomePA package (Yu and He 2016). In order to compare pathways activated by either THRSP silencing or insulin stimulation, we used a previously published microarray dataset (GSE26637, downloaded from <https://www.ncbi.nlm.nih.gov/geo/>) of human SAT collected during an euglycemic hyperinsulinemic clamp (Soronen et al. 2012). We used the data of 5 arrays, each generated from SAT of lean insulin-sensitive females collected at fasting and at 180 min of sustained hyperinsulinemia. Raw data (CEL files) were normalized by using the Robust Multichip Average (RNA) normalization function of the affy package (Gautier et al. 2004). Next, to determine the transcriptomic alterations in SAT induced by hyperinsulinemia with reference to fasting, DEG analyses were performed using the limma algorithm (Phipson et al. 2016). The DEG results then underwent probe set annotations using their corresponding chips and filtering for duplicated genes, of which the most significant probe was retained. Pathway analyses were subsequently performed using the ReactomePA package (Yu and He 2016). Significantly altered pathways were further compared between insulin resistance and THRSP silencing, and only the commonly altered pathways were selected.

Gene expression analysis

Quantitative real-time PCR (qPCR) was used to measure gene expression in the SGBS and 3T3-L1 adipocytes and human SAT. Total RNA from SGBS cells or from tissue biopsies was isolated using the Lipid Tissue Mini Kit (Qiagen; Gaithersburg, MD) according to the manufacturer's protocols. RNA from 3T3-L1 cells was isolated using PureLink™ RNA Mini Kit (Invitrogen, Carlsbad, CA; 12183018A). The SuperScript® VILO™ synthesis Kit (Invitrogen, Carlsbad, CA; 11754-050) was used

for reverse transcription of cDNA. To quantify mRNA expression, qPCR was performed using the LightCycler® SYBR-Green® master mix (Roche Diagnostics, Mannheim, Germany; 04887352001) and a LightCycler 480 II Real-Time PCR system (Roche Applied Science, Penzberg, Germany). For analysis, crossing point (Cp) values were calculated from amplification curves and normalized to Cp values of the housekeeping genes ribosomal protein lateral stalk subunit P0 (36B4) and actin. Sequences of the used qPCR primers are listed in Table 1 and mouse qPCR primers are listed in Additional file 1: Table S5.

Western blotting

SGBS and 3T3-L1 protein expressions were quantified by western blotting. Cells were lysed in RIPA buffer (15 mM Tris-HCl, pH 7.4, 1% NP40 1%, 1.25% sodium deoxycholate, 150 mM NaCl, 1 mM EDTA, 1% SDS). Equal amounts of protein were loaded on 10% SDS polyacrylamide gels (Fast Cast TGX Stain-Free, BioRad, Hercules, CA), and blotting was done on PVDF membranes using the BioRad Transblot system. The membranes were blocked and probed overnight with anti-THRSP (Proteintech; 13054-I-AP) in 5% milk in TBS, 0.5% Tween-20. Proteins were detected with enhanced chemiluminescence (Pierce ECL Western; Thermo Scientific, Waltham, MA; 32106). Image Lab (BioRad) was used to quantify the corresponding protein band intensities, which were normalized to total protein intensity.

Measurement of mitochondrial respiration

The mitochondrial oxygen consumption rate (OCR) in control and THRSP-silenced or overexpressing SGBS cells was measured using the Seahorse XF96 Extracellular Flux Analyzer (Agilent Technologies). SGBS preadipocytes were plated onto XF96 cell culture plates (Agilent Technologies), differentiated, and transfected as described above. The cells were incubated for 1 h in XF base medium with 10 mM D-(+)-glucose (Sigma; 68769), 1 mM sodium pyruvate (Sigma; S8636), and 2 mM L-glutamine (Gibco; 25030-024), in a CO₂ free incubator. OCR was measured using the XF Cell Mito

Stress Test Kit (Agilent Technologies) according to the manufacturer's protocol. Maximal respiration rates were obtained and normalized to cell count. Hoechst (3.3 μM; Thermo Scientific; 62249) was used to stain the cells, and the counting was done using the Cytation 5 Cell Imaging Multi-Mode Reader (Biotek, Agilent Technologies). OCR in THRSP-overexpressing and control cells was measured in preadipocytes due to a defective differentiation capacity of the lentivirally transduced cells on Seahorse plates. The overexpressing cells were seeded onto XF96 cell culture plates and grown until confluency, followed by the OCR measurement.

Measurement of fatty acid oxidation

The THRSP-silenced or overexpressing SGBS adipocytes were starved in a substrate-limited medium (Glucose-free DMEM [Gibco, 11966025]; 1 mM L-glutamine [Gibco, 25030-081]; 0.5 mM glucose) for 24 h. The next day, the cells were pre-treated for 3 h with 1 mM L-carnitine or 50 μM Etomoxir (EMD Millipore Corp. USA; 236020). Thereafter, the cells were incubated with [³H] oleic acid (0.1 μCi/well; Perkin Elmer; NET289005MC) and albumin-bound oleic acid (Sigma; 03008) in KH buffer (25.0 mM NaHCO₃, 1.2 mM MgSO₄ × 7H₂O, 1.2 mM KH₂PO₄, 4.7 mM KCl, 118.1 mM NaCl, 2.5 mM CaCl₂ × 2H₂O, 10 mM HEPES, pH7.4) for 2 h. The incubation medium was collected, and the samples were passed through OH⁻ ion exchange columns (Dowex 1X8-200 Ion Exchange Resin, 217,425, Merck). The flow-through was collected to scintillation vials, and the amount of oleate oxidized was determined from the radioactive water by liquid scintillation counting.

Glucose uptake

The THRSP-silenced or overexpressing SGBS adipocytes were washed carefully with PBS and starved in glucose- and serum-free DMEM for 24 h. The cells were treated with 100 nM insulin for 20 min and then incubated with 50 nM deoxy-D-glucose and [³H] deoxy-D-glucose (0.5 μCi/well; Perkin Elmer; NET328A250UC) for 5 min. Glucose uptake was terminated by three washes with ice-cold PBS. The cells were lysed with 0.1% SDS and radioactivity was measured by liquid scintillation counting.

Lipidomic analysis

Total lipids were extracted from THRSP-silenced and control mature SGBS adipocyte lysates by using the Bligh and Dyer method in the presence of naturally absent lipid species as internal standards (Bligh and Dyer 1959). The following lipid species were added as internal standards: cholesterol ester (CE) 17:0, CE 22:0, ceramide (Cer) 18:1;O2/14:0, Cer 18:1;O2/17:0, diglyceride (DG) 14:0/14:0, DG 20:0/20:0, free cholesterol

Table 1 Sequences of primers used for qPCR analysis

Primer name	Sequence
36B4 F	5'-CATGCTCAACATCTCCCTT-3'
36B4 R	5'-GGGAAGGTGTAATCCGTCTCC-3'
Actin F	5'-GACAGGATGCAGAAGGAGATT-3'
Actin R	5'-TGATCCACATCTGCTGGAAGG-3'
THRSP F	5'-CAGGTGCTAACCAAGCGTTAC-3'
THRSP R	5'-CAGAAGGCTGGGGATCATCA-3'

(FC) [D7], lyso-phosphatidylcholine (LPC) 13:0/0:0, LPC 19:0/0:0, lyso-phosphatidylethanolamine (LPE) 13:0/0:0, PC 14:0/14:0, phosphatidylcholine (PC) 22:0/22:0, phosphatidylethanolamine (PE) 14:0/14:0, PE 20:0/20:0 (di-phytanoyl), phosphatidylglycerol (PG) 14:0/14:0, PG 20:0/20:0 (di-phytanoyl), phosphatidylinositol (PI) 17:0/17:0, phosphatidylserine (PS) 14:0/14:0, PS 20:0/20:0 (di-phytanoyl), sphingomyelin (SM) 18:1;O2/12:0, triglyceride (TG) 17:0/17:0/17:0, and TG 19:0/19:0/19:0. The lipid extract was recovered by a pipetting robot (Tecan Genesis RSP 150) and vacuum dried. The residues were dissolved in 7.5 mM ammonium acetate in methanol/chloroform (3:1, v/v) for low mass resolution tandem mass spectrometry and chloroform/methanol/2-propanol (1:2:4 v/v/v) with 7.5 mM ammonium formate for high resolution mass spectrometry.

The analysis of lipids was performed by direct flow injection analysis (FIA) using a triple quadrupole mass spectrometer (FIA-MS/MS; QQQ triple quadrupole) and a hybrid quadrupole-Orbitrap mass spectrometer (FIA-FTMS; high mass resolution). FIA-MS/MS (QQQ) was performed in positive ion mode using the analytical setup and strategy described previously (Liebisch et al. 2004). A fragment ion of m/z 184 was used for LPC (Liebisch et al. 2002). The following neutral losses were applied: PE and LPE 141, PS 185, PG 189 and PI 277 (Matyash et al. 2008). PE-based plasmalogens (PE P) were analyzed according to the principles described by Zemski-Berry (Zemski Berry and Murphy, 2004). Sphingosine based Cer and HexCer were analyzed using a fragment ion of m/z 264 (Liebisch et al. 1999). Quantification was achieved by calibration lines generated by addition of naturally occurring lipid species to the respective sample matrix.

A detailed description of the FIA-FTMS strategy was published recently (Höring et al. 2021, 2020). TG, DG, and CE were recorded as $[M + NH_4]^+$ in positive ion mode in range m/z 500–1000 for 1 min with a maximum injection time of 200 ms, an automated gain control of 1×10^6 , three microscans and a target resolution of 140,000 (at m/z 200). PC, phosphatidylcholine ether and SM were analyzed as $[M + HCOO]^-$ in negative ion mode in range m/z 520–960 at the same resolution setting. Multiplexed acquisition was applied for the $[M + NH_4]^+$ of FC and the corresponding internal standard (FC[D7]) (Höring et al. 2019). Quantification was performed by multiplication of the spiked internal standard amount with analyte-to-internal standard ratio. Lipid species were annotated according to the latest proposal for shorthand notation of lipid structures that are derived from mass spectrometry (Liebisch et al. 2020).

Statistical methods

Normality of the data was tested using the Shapiro Wilk's test. The independent 2-sample 2-tailed Student's t -test or the Mann–Whitney U test were used to compare two groups, whereas the one-way ANOVA or the Kruskal–Wallis test were employed to compare three or more groups of normally and non-normally distributed data, respectively. The Spearman's correlation coefficient was used to determine bivariate correlations. Multiple Mann–Whitney U tests with FDR set to 5% were used to compare means of the lipidomic data. Data are in mean \pm SD. A P value ≤ 0.05 was considered statistically significant. Statistical analyses were performed with GraphPad Prism 9.3.1 (GraphPad Software, Inc., La Jolla, CA, USA) or R 4.0.3.

Results

THRSP is induced by insulin in human adipocytes in vivo and in vitro

Clinical characteristics of the subjects are shown in Table 2 ($n=36$). Mean M-value for all subjects was 6.4 mg/kgBW/min, with SD of 1.8 mg/kgBW/min. Insulin induced *THRSP* expression in human SAT in a time-dependent manner (Fig. 1a). The induction by insulin was stronger in more insulin-sensitive subjects and *THRSP* expression correlated positively with the M-value, which is a measure of insulin sensitivity ($r_{360 \text{ min}}=0.62$; $P<0.0001$; Fig. 1b, c). Moreover, clinical features associated with insulin resistance, such as the waist-to-hip ratio, SAT volume, serum insulin and C-peptide concentrations, and fasting plasma glucose concentrations, correlated inversely with *THRSP* expression (Fig. 1d).

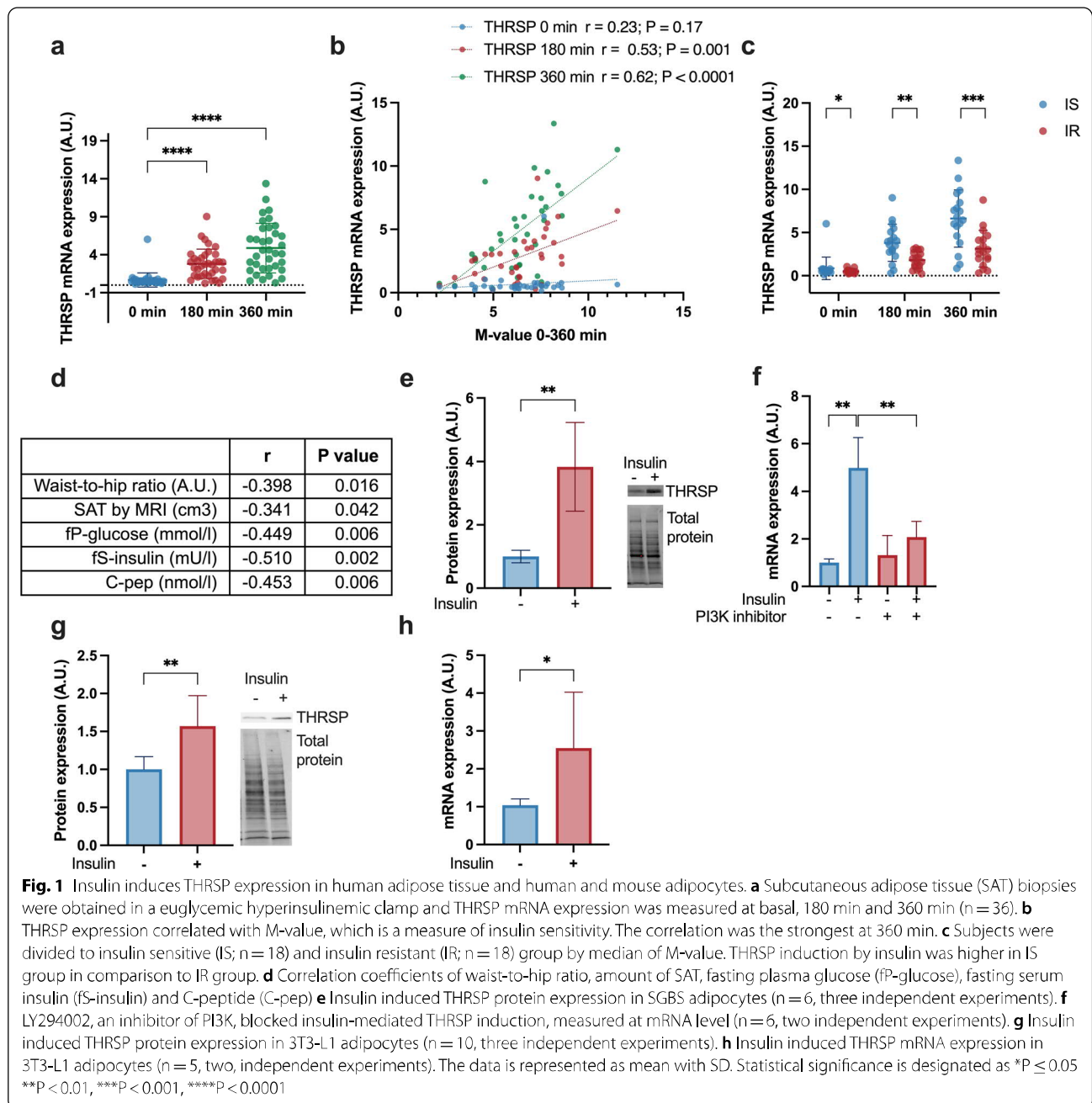
To confirm that the insulin induction of *THRSP* occurs in adipocytes and also affects *THRSP* protein

Table 2 Clinical characteristics of the participants subjected to euglycemic hyperinsulinemic clamp

	All (n = 36)	IS (n = 18)	IR (n = 18)
Age (years) ^a	40 \pm 9	38 \pm 8	43 \pm 11
Weight (kg) ^a	75 \pm 15	69 \pm 11	80 \pm 16
BMI (kg/m ²) ^a	27.3 \pm 5.0	24.9 \pm 3.7	29.8 \pm 5.0
Postmenopausal (n)	6	1	5
Waist-to-hip ratio (A.U.) ^a	0.9 \pm 0.1	0.8 \pm 0.0	0.9 \pm 0.1
fP-glucose ^b (mmol/l) ^a	5.2 \pm 0.6	5.0 \pm 0.7	5.4 \pm 0.5
fS-insulin ^c (mU/l) ^a	4.1 \pm 1.6	3.5 \pm 1.2	4.8 \pm 1.7
M-value ^d (mg/kgBW/min) ^a	6.4 \pm 1.8	7.8 \pm 1.1	5.0 \pm 1.2
Body fat (%) ^a	32.9 \pm 7.2	30.1 \pm 7.2	35.7 \pm 6.2
SAT by MRI (cm ³) ^a	4111 \pm 2189	2893 \pm 1517	5328 \pm 2103
C-peptide (nmol/l) ^a	0.58 \pm 0.18	0.51 \pm 0.11	0.66 \pm 0.20

^a Data is represented as average \pm SD

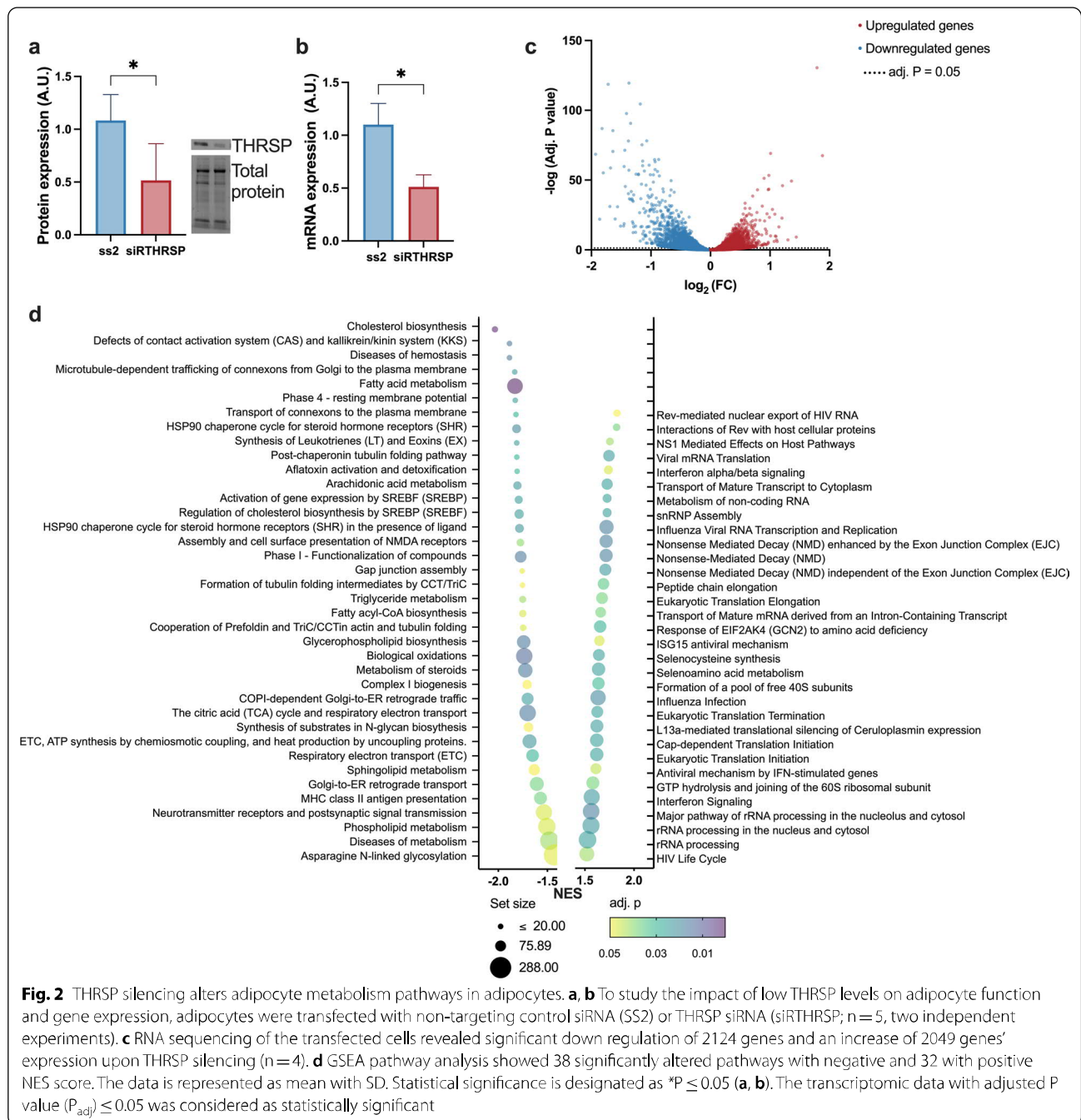
^b fP, fasting plasma; ^cfS, fasting serum; ^dBW, body weight



levels, mature human SGBS adipocytes were treated with insulin. Indeed, insulin significantly increased both THRSP mRNA and protein concentrations of the adipocytes (Fig. 1e, f). Addition of the PI3K inhibitor LY294002 (LY) abolished *THRSP* induction, suggesting that insulin regulates *THRSP* in a PI3K-dependent manner (Fig. 1f). THRSP induction by insulin was also confirmed in another cell model, 3T3-L1 adipocytes (Fig. 1g, h).

THRSP silencing alters metabolic pathways

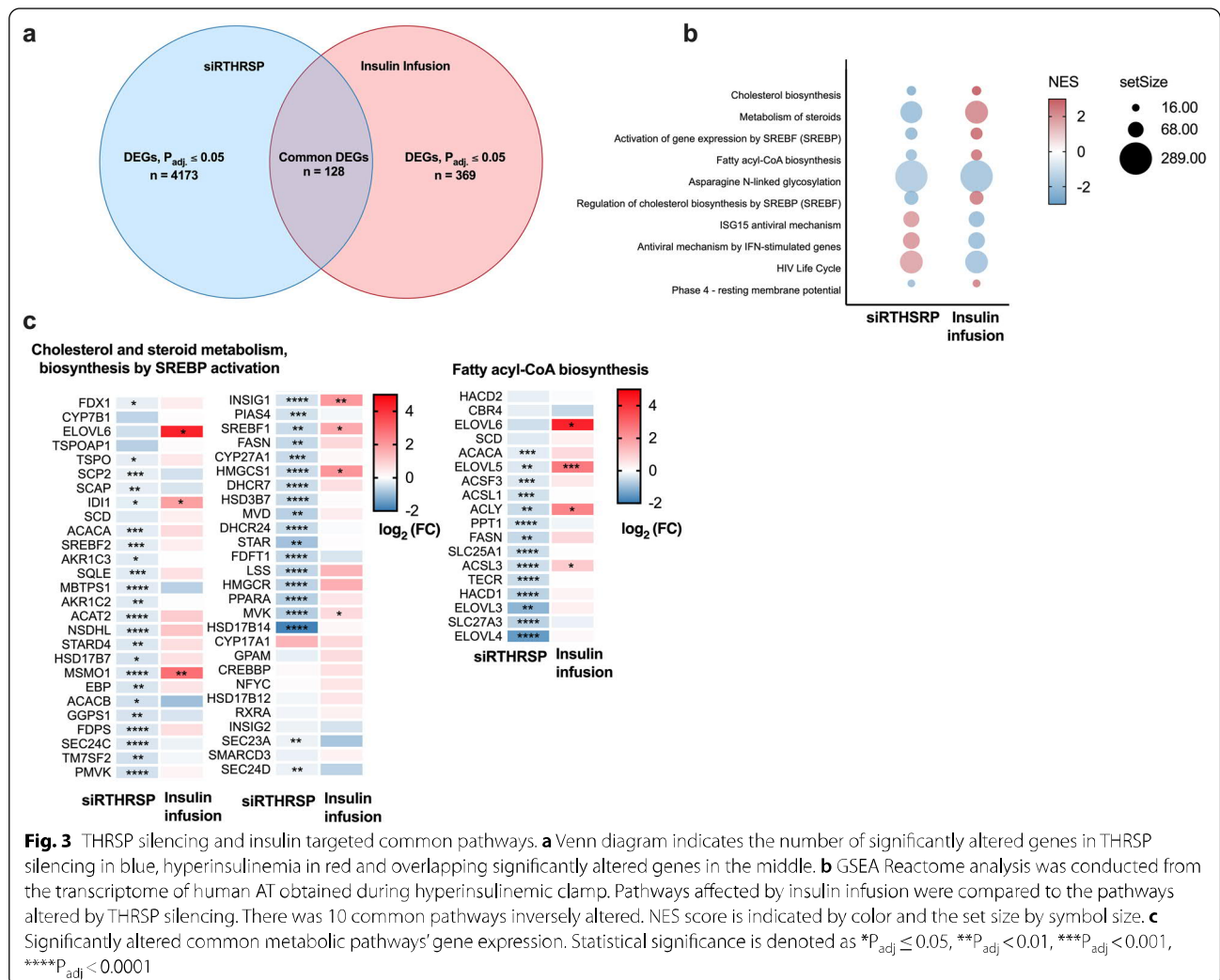
To identify putative functions of THRSP, we performed a transcriptomic analysis by next-generation RNA sequencing in THRSP-silenced SGBS adipocytes. Silencing efficiency was 52% at the protein level and 49% at the mRNA level (Fig. 2a, b). Of the over 27,000 total transcripts detected, those significantly differentially expressed numbered 4174 ($P_{adj} \leq 0.05$; Fig. 2c). Expression data for the differentially expressed genes (DEGs) is shown in Additional file 2: Table S1. A gene set



enrichment analysis (GSEA) revealed that multiple pathways involved in energy and lipid metabolism (cholesterol biosynthesis, fatty acid metabolism, citric acid cycle, steroid metabolism, and sphingolipid metabolism) had a negative normalized enrichment score (NES), indicating genes in those pathways to be mostly suppressed by THRSF silencing (Fig. 2d).

As we found *THRSF* to be an insulin-inducible gene, a further analysis was performed to understand which

insulin-mediated functions in human SAT are altered in response to THRSF silencing. A publicly available microarray dataset (GSE26637) from our previous study was used to identify differentially expressed genes in AT during euglycemic hyperinsulinemia, and the altered gene profile was then compared with transcriptomic changes in the THRSF-silenced SGBS adipocytes. A total of 128 common DEGs were identified between the datasets (Fig. 3a; gene list in Additional file 1: Table S2). Several



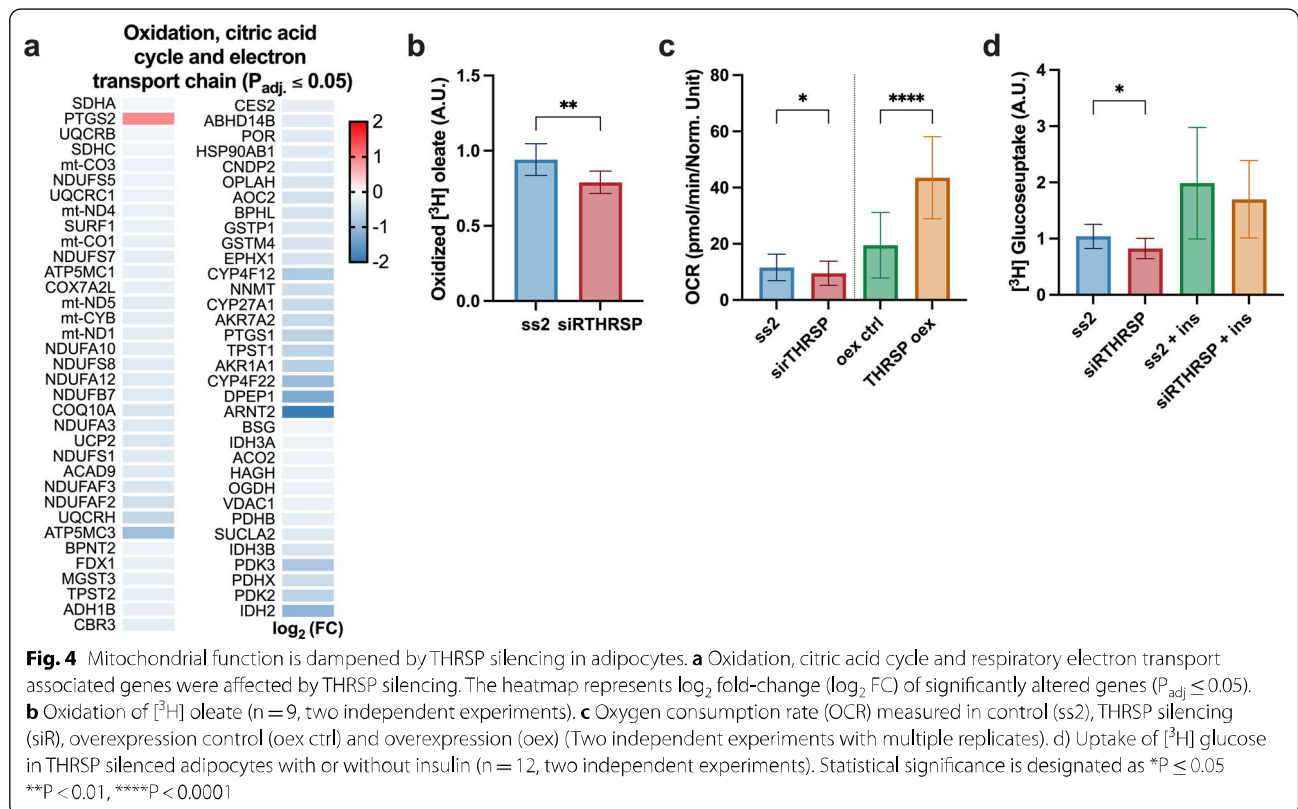
common and inversely affected pathways were identified by a Reactome GSEA (Fig. 3b). These included steroid metabolism, cholesterol biosynthesis, fatty acid biosynthesis, and SREBP-regulated pathways, suggesting that THRSR might be an important mediator of these functions of insulin in adipocytes. Gene expressions of the altered metabolic pathways are shown in Fig. 3c.

THRSR silencing impairs mitochondrial function

In THRSR-silenced adipocytes, genes involved in the citric acid cycle, oxidative phosphorylation, and oxidation were significantly downregulated (Fig. 4a, Additional file 1: Fig. S2c). Thus, we next assessed whether THRSR silencing affects mitochondrial functions. By employing radioactive oleate as a substrate, we found fatty acid oxidation to be significantly decreased in THRSR-silenced cells as compared to SS2 controls (Fig. 4b; $P = 0.0037$). To study mitochondrial respiration, the mitochondrial oxygen consumption rate

(OCR) was measured using the Seahorse Mito Stress test. THRSR silencing in mature adipocytes led to significantly decreased maximal OCR (Fig. 4c; $P = 0.035$), whereas overexpression of THRSR in preadipocytes markedly increased OCR (Fig. 4c; < 0.0001). To determine whether the decreased mitochondrial activity is due to dampened mitochondrial biogenesis rather than mitochondrial function, we measured the ratio of mitochondrial DNA to genomic DNA. The ratio remained unchanged by THRSR silencing, implying that there was no inhibition of mitochondrial biogenesis (Additional file 1: Fig. S1).

To investigate if the dampened oxidative phosphorylation (as measured by OCR) is related to altered glucose uptake, we next measured the uptake of radioactive glucose in THRSR-silenced adipocytes. THRSR silencing decreased the uptake of glucose in comparison to SS2 controls ($P = 0.03$), but a similar change was not observable during treatment of the cells with insulin (Fig. 4d).



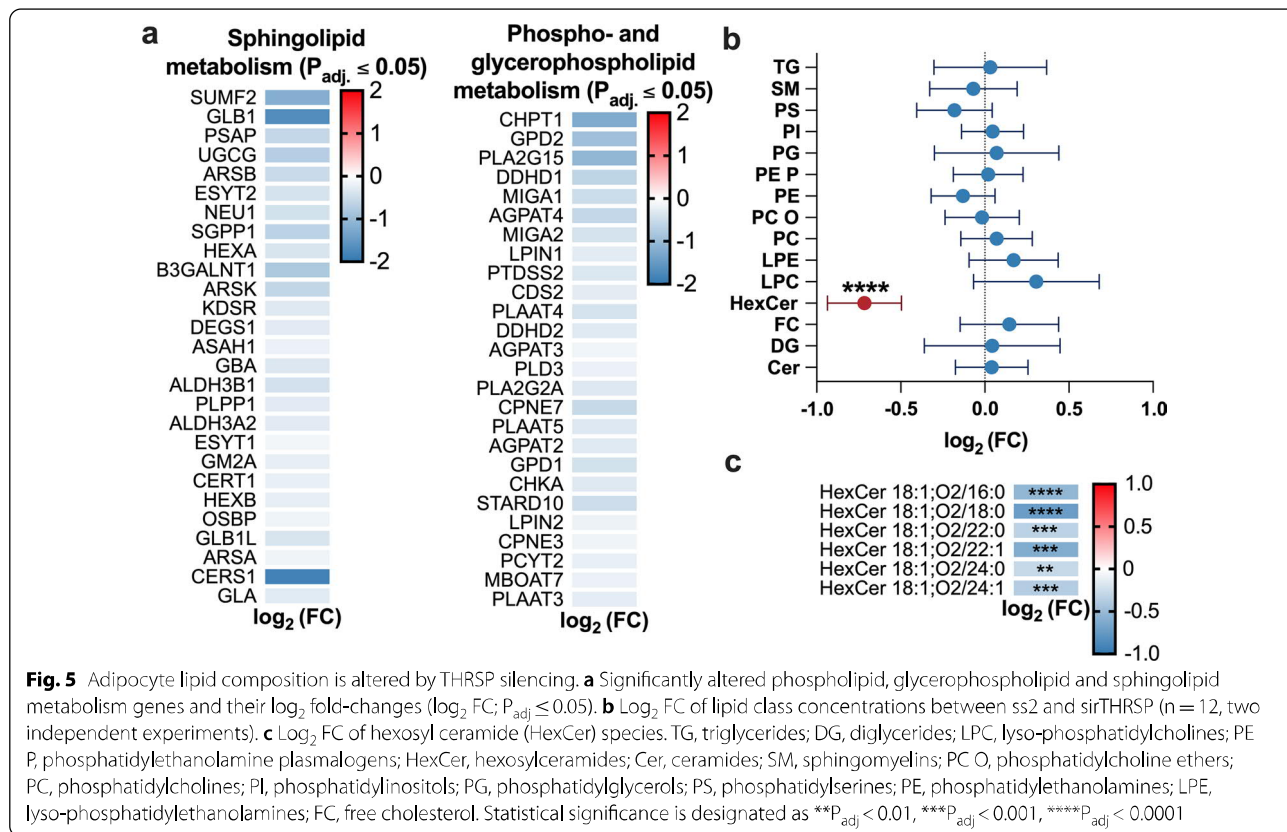
THRSP silencing alters the lipid composition in adipocytes

THRSP reportedly has a lipogenic function in various tissues, and the observed impairment of mitochondrial function during its silencing shows that THRSP regulates adipocyte energy metabolism (Freake and Oppenheimer 1987; Jump et al. 1984; Kinlaw et al. 1995). Moreover, the transcriptomic analysis suggested a potential role of THRSP in cholesterol, phospholipid, glycerophospholipid, and sphingolipid metabolism (Fig. 5a; cholesterol metabolism in Fig. 3c). We next performed a lipidomic analysis of THRSP-silenced adipocytes, which showed a significant reduction in the total concentrations of hexosylceramides (HexCer) compared to controls (Fig. 5b). Specifically, concentrations of HexCer species 18:1; $O_2/16:0$, 18:1; $O_2/18:0$, 18:1; $O_2/22:0$, 18:1; $O_2/22:1$, 18:1; $O_2/24:0$, and 18:1; $O_2/24:1$ were reduced (Fig. 5c, all lipid species shown in Additional file 1: Table S3). Corroborating these findings, the transcriptomic analysis revealed alterations in key genes regulating glycerophospho- and glycosphingolipid metabolism. In the glycosyl ceramide pathway, the key gene UDP-glucose ceramide glucosyltransferase (*UGCG*), which catalyzes the glycosylation of ceramides to glucosylceramides, was down-regulated. Subsequently, downstream genes converting glucosylceramides to more complex glycosphingolipids were inhibited. Genes involved in the de novo synthesis

of ceramides were also inhibited, including dihydroceramide desaturase (*DEGS1*) and ceramide synthases 1 and 4 (*CerS1*; -4; Fig. 6). Consistent with our observations in human adipocytes, genes involved in sphingolipid metabolism were down-regulated in THRSP-silenced 3T3-L1 adipocytes as well (Additional file 1: Fig. S2c). Interestingly, when THRSP-silenced adipocytes with HexCer defect were treated with exogenous glucosylceramides, the mitochondrial respiration was restored (Additional file 1: Fig. S3).

Discussion

In the present study, we investigated functions of the insulin-regulated gene product, THRSP, by employing human SAT biopsies and cultured human adipocytes. We studied the expression of THRSP before and during euglycemic hyperinsulinemia in vivo and found that insulin significantly induced THRSP expression, which was enhanced in subjects with high insulin sensitivity. A transcriptomic analysis of THRSP-silenced adipocytes revealed altered expression of genes not only related to lipid metabolism but also to mitochondrial function, oxidative phosphorylation, and oxidation pathways. Further analyses in cultured human SGBS adipocytes provided evidence for functions of THRSP in maintaining mitochondrial activity, fatty acid oxidation, and normal



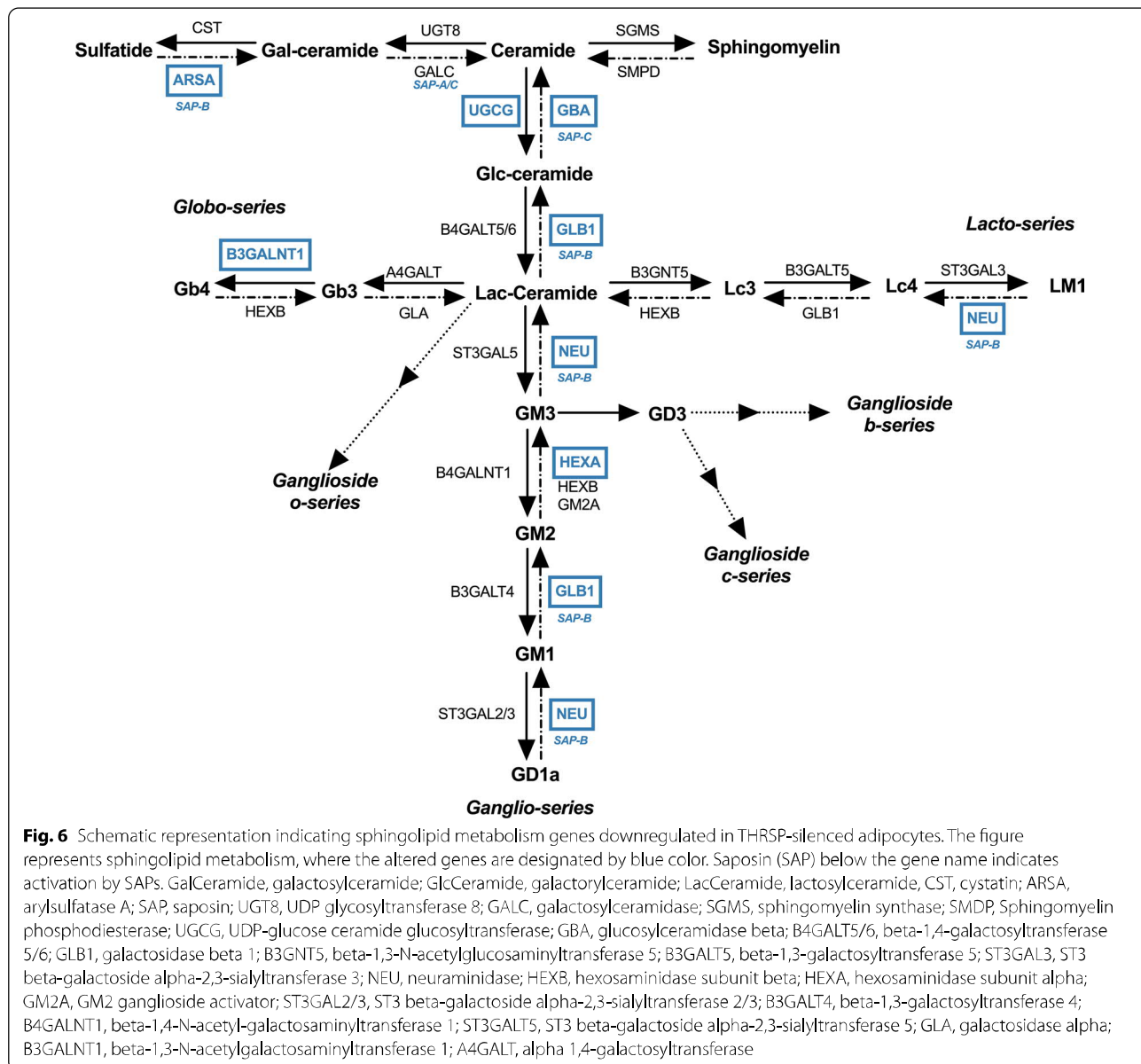
cellular sphingolipid concentrations, with a marked reduction of HexCer in THRSP-silenced adipocytes.

Our observations on the induction of THRSP by insulin are in agreement with the previously known lipogenic function of the protein (Freake and Oppenheimer 1987; Wu et al. 2013). A comparative transcriptomic analysis revealed that, in both THRSP-silenced adipocytes and insulin-stimulated AT, commonly affected genes belonged to the ‘Lipid metabolism’ and ‘SREBP-activated’ pathways—SREBP activity playing a crucial role in adipocyte lipogenesis (Gondret et al. 2001; Kim and Spiegelman, 1996). The above observations support a function of THRSP as a regulator of lipid homeostasis, while possibly mediating the effects of insulin on adipocyte lipid metabolism. Moreover, antiviral interferon-stimulated gene expression pathways were shared between adipocyte THRSP silencing and AT insulin induction in vivo. Interferon signaling in adipocytes is known to significantly affect adipocyte differentiation, lipogenesis, and immune responses (Lee et al. 2016; McGillicuddy et al. 2009; Wensveen et al. 2015). The downregulation of interferon-stimulated genes by insulin and THRSP might thus contribute to the enhanced insulin-mediated lipogenesis in adipocytes. However, a contradicting report claims that interferon signaling can improve metabolic

dysfunction in AT (Wieser et al. 2018). Further studies are warranted to understand the insulin-mediated regulation of interferon signaling and how it regulates adipocyte lipid metabolism.

We observed quite a low number of pathways that were commonly regulated by insulin in AT in vivo and in adipocytes subjected to THRSP silencing. It is, however, worth noting that the method of differential expression analysis was different in the two datasets: next-generation RNA-seq was employed in the THRSP-silenced cells while microarrays were used in the in vivo study. This difference in technology might limit the number of pathways shared between the studies. On the other hand, the high number of genes and pathways affected by THRSP silencing may indicate that THRSP in adipocytes could execute additional insulin-independent functions that are crucial for AT metabolism. Therefore, a further effort was made to understand the functions of THRSP in adipocyte metabolism.

The RNA-seq and pathway analysis in THRSP-silenced cells revealed significant regulation of several mitochondrial functions, with alterations in key genes involved in oxidative phosphorylation and the TCA cycle (Fig. 4a). Mitochondrial function is generally dampened in obese AT, and this is often referred to as a hallmark of obesity



(Schöttl et al. 2015; Vernochet et al. 2014). Of interest, a previous study has shown that THRSP expression is decreased in obesity (Ortega et al. 2010). Contrary to this finding, we did not observe a significant difference in THRSP expression between IS and IR subjects in the basal state, possibly due to the limited range of BMI among our study participants. Mitochondrial respiration was dampened, however, in adipocytes subjected to THRSP silencing. Despite the relatively low abundance of mitochondria in white adipocytes they are essential for the cells' metabolic functions, and mitochondrial dysfunction does contribute to AT inflammation (Woo et al. 2019).

Thyroid hormone receptor signaling has been suggested to increase the trafficking of fatty acids into mitochondria (Sayre and Lechleiter, 2012). Since THRSP is also a T3-induced gene, it could be surmised to play a role in this process. Previous studies have shown that thyroid hormones induce enzymes favoring fatty acid oxidation, such as the uncoupling protein 2 (UCP2) (Sinha et al. 2018), which showed reduced expression in our THRSP-silenced adipocytes. Even though mitochondrial respiration and fatty acid oxidation was reduced upon THRSP silencing, the expression of CD36 was unaltered, and carnitine palmitoyltransferase 1A (CPT1a) expression was increased. However, the expression of fatty acid-binding

proteins 3 and 7 (FABP3, -7) was decreased, suggesting an impaired influx of fatty acids into the cells, which putatively contributes to the reduced fatty acid oxidation. The observed reduction in OCR in the THRSP-silenced cells could also reflect a reduced glucose disposal rate (Woerle et al. 2003). While the reduction in OCR may in part be due to decreased glucose uptake, THRSP could also play a direct role in the regulation of oxidative phosphorylation, as suggested by our transcriptomic analysis. In alignment with our observations, THRSP was identified as a sirtuin 1-regulated gene in 3T3-L1 adipocytes, sirtuins being established regulators of mitochondrial function and biogenesis in human adipocytes (Majeed et al. 2021).

In addition to the direct effects on mitochondrial function, we observed that THRSP silencing significantly altered the adipocyte lipid composition. Several studies have shown that obesity and its metabolic consequences are closely related to disruptions in sphingolipid metabolism (Chaurasia et al. 2016; Green et al. 2021). Moreover, altered sphingolipid metabolism is connected to dysfunction of mitochondria (Knupp et al. 2017; Roszczyk-Owsiejczuk and Zabielski 2021). To this end, we observed a reduction in HexCer (glucosyl- and galactosylceramides) in the THRSP-silenced cells. Consistent with these changes, genes involved in the synthesis of glucosylceramides were downregulated (Fig. 6), including UDP-glucose ceramide glucosyltransferase (*UGCG*), the enzyme converting ceramide to glucosylceramide, as well as β -galactosidase (*GLBI*), neuraminidase 1 (*NEUI*), and hexosaminidase α (*HEXA*), which convert gangliosides back to glucosylceramide. In addition to reduced concentrations of HexCer, the downregulation of these enzymes could theoretically lead to an accumulation of ceramides and GM1, -2, and -3 gangliosides, all of which have been identified as contributors of insulin resistance in various cell types (Demir et al. 2020; Haynes et al. 2012; Kajihara et al. 2020; Lipina and Hundal, 2015; Sasaki et al. 2018; Wang et al. 2014; Yamashita et al. 2003). However, ceramide concentrations were not significantly increased, possibly due to the observed downregulation of ceramide synthases.

Interestingly, Chew et al. found HexCer plasma concentrations to negatively correlate with BMI and HOMA-IR, whereas ceramides showed a positive correlation (Chew et al. 2019). HexCer are known to play a role in resolving AT inflammation. They are presented by antigen-presenting cells as endogenous lipid antigens, resulting in iNKT cell activation and subsequent clearing of inflammation and the associated AT dysfunction (Lynch et al. 2012; Park et al. 2019; Rakhshandehroo et al. 2019; van Eijkeren et al. 2020, 2018). Although several publications have found sphingolipids as a whole to contribute

to mitochondrial dysfunction, there is recent evidence that *UGCG* increases glycolysis and oxidative phosphorylation (Schömel et al. 2020). Supporting this finding, we observed that addition of exogenous glucosyl ceramide rescued the mitochondrial respiration in adipocytes subjected to THRSP silencing. Although addition of exogenous glucosylceramides does not rescue all of the alterations in lipid profile in THRSP-silenced adipocytes, it supports the notion that THRSP may impact mitochondrial functions both via the expression of genes involved in mitochondrial function and by regulating sphingolipid metabolism. Suppression of *UGCG* expression and the reduction in HexCer could thus be linked to impaired mitochondrial metabolism.

We also observed a reduction in the mRNA of several lysosomal hydrolases or their regulators, including arylsulfatase A, B, and K, choline phosphotransferase, and prosaposin. Prosaposin is a precursor of saposin, which is an activator of sulfatases in the sphingolipid metabolism. Deficiencies in these enzymes are linked to lysosomal storage disorders, but data is limited regarding their role in adipocyte metabolism or obesity (Allende et al. 2021; Monteith et al. 2016; Raj et al. 2020; Simonis et al. 2019; Tomanin et al. 2018; Trabszo et al. 2020). Lysosomal storage disorders are often associated with mitochondrial dysfunction, altered metabolism and fibrosis, showing parallels with obesity (Mizunoe et al. 2019; Pshezhetsky, 2015). Therefore, it might be of interest to study a possible role of THRSP in lysosomal storage diseases.

THRSP is regulated by insulin, thyroid hormone, carbohydrate intake, and fatty acids (LaFave et al. 2006). The present RNA-seq data suggest that, although insulin does induce THRSP, manipulation of either THRSP expression or insulin levels affected partly distinct pathways. In light of the present observations, we speculate that THRSP could execute distinct functions depending on the regulator that induces it. For instance, regulation of mitochondrial function could be a thyroid hormone-induced function of THRSP (Comas et al. 2019; Lanni et al. 2016). This is supported by the finding that mitochondrial pathways were not among the commonly regulated ones between AT insulin induction in vivo and the THRSP-silenced adipocytes. Moreover, non-coding RNA processing was identified as being potentially inhibited by THRSP, independent of insulin action. This aligns with previous research demonstrating that T3 inhibits various long non-coding RNAs in hepatocellular cancer—this inhibition could thus be mediated via THRSP (Huang et al. 2021).

Collectively, our findings shed light on the functions of THRSP in human AT in vivo and adipocytes in vitro, suggesting that THRSP plays a major role in the regulation of adipocyte metabolism via altering both

mitochondrial function and cellular lipid composition. The present work adds to the existing knowledge, emphasizing the impact THRSP may have on whole-body health and development of metabolic disease. Fluctuations in THRSP expression might represent a physiologic response to nutritional and hormonal stimuli, which are known to be disturbed in obesity and metabolic disease. Thus, further studies are warranted to investigate whether restoring of THRSP responsiveness in insulin-resistant individuals could have therapeutic potential for ameliorating metabolic disease.

Abbreviations

AT: Adipose tissue; BMI: Body mass index; Cer: Ceramides; DG: Diglycerides; DEG: Differentially expressed gene; FC: Free cholesterol; GSEA: Gene set enrichment analysis; HexCer: Hexosylceramides; LPC: Lyso-phosphatidylcholines; LPE: Lyso-phosphatidylethanolamines; NES: Normalized enrichment score; OCR: Oxygen consumption rate; PC: Phosphatidylcholines; PC O: Phosphatidylcholine ethers; PE: Phosphatidylethanolamines; PE P: Phosphatidylethanolamine plasmalogens; PG: Phosphatidylglycerols; PI: Phosphatidylinositols; PI3K: Phosphoinositide 3-kinase; PS: Phosphatidylserines; SAT: Subcutaneous adipose tissue; SGBS: Simpson-Golabi-Behmel syndrome (cells); SM: Sphingomyelins; TG: Triglycerides.

Supplementary Information

The online version contains supplementary material available at <https://doi.org/10.1186/s10020-022-00496-3>.

Additional file 1. Supplementary methods, Table S2–S5, Fig. S1–S3.

Additional file 2. Table S1.

Acknowledgements

We thank Eija Pirinen for insightful discussion and techniques for studying mitochondria, and Riikka Kosonen, Päivi Ihamuotila and Aila Karioja-Kallio for their superb technical assistance.

Author contributions

MAA: Conceptualization, methodology, analysis, writing; MH: methodology, analysis; VDN: methodology, analysis; SQ: reviewing and editing; JHT: methodology, analysis; MN: methodology, analysis; MW: resources, editing; PFP: resources, editing; YZ: methodology, analysis; GL: resources, methodology; PANH: supervision, conceptualization, writing; HYJ: resources, reviewing and editing; VMO: supervision, conceptualization, writing. All authors read and approved the final manuscript.

Funding

This study was supported by the Kyllikki and Uolevi Lehtikainen Foundation (MAA), the Emil Aaltonen Foundation (MAA), the Liv och Hälsa Foundation (VMO), the Diabetes Research Foundation (VMO), Diabetes Wellness Finland (VMO), and the Jane and Aatos Erkko Foundation (VMO). MAA has a salaried position from Doctoral Programme in Clinical Research, University of Helsinki. PFP was supported by the Deutsche Forschungsgemeinschaft—project number 398707781—Heisenberg professorship.

Availability of data and materials

Transcriptomic and lipidomic data of THRSP-silenced adipocytes are included in this article and its additional information files. Publicly available microarray data of SAT (GSE26637) can be downloaded from <https://www.ncbi.nlm.nih.gov/geo/>. Other data are available on reasonable request.

Declarations

Ethics approval and consent to participate

Each participant provided a written informed consent after being explained the nature and potential risks of the study, which received approval from the Ethics Committee of the Hospital District of Helsinki and Uusimaa (Helsinki, Finland).

Consent for publication

Not applicable.

Competing interests

The authors declare that they have no competing interests.

Author details

¹Minerva Foundation Institute for Medical Research, Biomedicum 2U, Tukholmankatu 8, 00290 Helsinki, Finland. ²Doctoral Programme in Clinical Research, University of Helsinki, Helsinki, Finland. ³Institute of Clinical Chemistry and Laboratory Medicine, University Hospital Regensburg, Regensburg, Germany. ⁴Division of Pediatric Endocrinology and Diabetes, Department of Pediatrics and Adolescent Medicine, University Medical Center Ulm, Ulm, Germany. ⁵Systems Immunity University Research Institute, and Division of Infection and Immunity, Cardiff University, Cardiff, UK. ⁶Department of Medicine, University of Helsinki and Helsinki University Hospital, Helsinki, Finland. ⁷Department of Anatomy, Faculty of Medicine, University of Helsinki, Helsinki, Finland.

Received: 18 February 2022 Accepted: 8 June 2022

Published online: 17 June 2022

References

- Ahonen MA, Asghar MY, Parviainen SJ, Liebisch G, Höring M, Leidenius M, Fischer-Posovszky P, Wabitsch M, Mikkola TS, Törnquist K, Savolainen-Peltonen H, Haridas PAN, Olkkonen VM. Human adipocyte differentiation and composition of disease-relevant lipids are regulated by miR-221–3p. *Biochim Biophys Acta Mol Cell Biol Lipids*. 2021. <https://doi.org/10.1016/j.bbali.2020.158841>.
- Allende ML, Zhu H, Kono M, Hoachlander-Hobby LE, Huso VL, Proia RL. Genetic defects in the sphingolipid degradation pathway and their effects on microglia in neurodegenerative disease. *Cell Signal*. 2021;78: 109879. <https://doi.org/10.1016/j.cellsig.2020.109879>.
- Anders S, Pyl PT, Huber W. HTSeq—a Python framework to work with high-throughput sequencing data. *Bioinformatics*. 2015;31:166–9. <https://doi.org/10.1093/bioinformatics/btu638>.
- Anderson GW, Zhu Q, Metkowsky J, Stack MJ, Gopinath S, Mariash CN. The Thrsp null mouse (Thrsptm1cnm) and diet-induced obesity. *Mol Cell Endocrinol*. 2009;302:99–107. <https://doi.org/10.1016/j.mce.2009.01.005>.
- Andrews S. Babraham Bioinformatics—FastQC A Quality Control tool for High Throughput Sequence Data [WWW Document]. 2020. URL <https://www.bioinformatics.babraham.ac.uk/projects/fastqc/> (accessed 1.21.22).
- Bligh EG, Dyer WJ. A rapid method of total lipid extraction and purification. *Can J Biochem Physiol*. 1959;37:911–7. <https://doi.org/10.1139/o59-099>.
- Bolger AM, Lohse M, Usadel B. Trimmomatic: a flexible trimmer for Illumina sequence data. *Bioinformatics*. 2014;30:2114–20. <https://doi.org/10.1093/bioinformatics/btu170>.
- Cao ZP, Wang SZ, Wang QG, Wang YX, Li H. Association of Spot14a gene polymorphisms with body weight in the chicken. *Poult Sci*. 2007;86:1873–80. <https://doi.org/10.1093/ps/86.9.1873>.
- Chaurasia B, Kaddai VA, Lancaster GI, Henstridge DC, Sriram S, Galam DLA, Gopalan V, Prakash KNB, Velan SS, Bulchand S, Tsong TJ, Wang M, Siddique MM, Yuguang G, Sigmundsson K, Mellet NA, Weir JM, Meikle PJ, Bin M, Yassin MS, Shabbir A, Shayman JA, Hirabayashi Y, Shiow SATE, Sugii S, Summers SA. Adipocyte ceramides regulate subcutaneous adipose browning, inflammation, and metabolism. *Cell Metab*. 2016;24:820–34. <https://doi.org/10.1016/j.cmet.2016.10.002>.
- Chen YT, Tseng PH, Tseng FY, Chi YC, Han DS, Yang WS. The serum level of a novel lipogenic protein Spot 14 was reduced in metabolic syndrome. *PLoS ONE*. 2019. <https://doi.org/10.1371/journal.pone.0212341>.

- Chew WS, Torta F, Ji S, Choi H, Begum H, Sim X, Khoo CM, Yin E, Khoo H, Ong W-Y, Van Dam RM, Wenk MR, Shyong Tai E, Herr DR. Clinical medicine large-scale lipidomics identifies associations between plasma sphingolipids and T2DM incidence. *JCI Insight*. 2019. <https://doi.org/10.1172/jci.insight.126925>.
- Comas F, Lluch A, Sabater M, Latorre J, Ortega F, Ricart W, López M, Fernández-Real JM, Moreno-Navarrete JM. Adipose tissue TSH as a new modulator of human adipocyte mitochondrial function. *Int J Obes (Lond)*. 2019;43:1611–9. <https://doi.org/10.1038/S41366-018-0203-1>.
- DeFronzo RA, Tobin JD, Andres R. Glucose clamp technique: a method for quantifying insulin secretion and resistance. *Am J Physiol Endocrinol Metab Gastrointest Physiol*. 1979. <https://doi.org/10.1152/ajpendo.1979.237.3.e214>.
- Demir SA, Timur ZK, Ateş N, Martínez LA, Seyrantepe V. GM2 ganglioside accumulation causes neuroinflammation and behavioral alterations in a mouse model of early onset Tay-Sachs disease. *J Neuroinflammation*. 2020. <https://doi.org/10.1186/S12974-020-01947-6>.
- Dobin A, Davis CA, Schlesinger F, Drenkow J, Zaleski C, Jha S, Batut P, Chaisson M, Gingeras TR. STAR: ultrafast universal RNA-seq aligner. *Bioinformatics*. 2013;29:15–21. <https://doi.org/10.1093/BIOINFORMA/TICS/BTS635>.
- Durinck S, Spellman PT, Birney E, Huber W. Mapping identifiers for the integration of genomic datasets with the R/bioconductor Package biomaRt. *Nat Protoc*. 2009. <https://doi.org/10.1038/nprot.2009.97>.
- Fischer-Posovszky P, Newell FS, Wabitsch M, Tornqvist HE. Human SGBS cells—a unique tool for studies of human fat cell biology. *Obes Facts*. 2008;1:184–9. <https://doi.org/10.1159/000145784>.
- Freake HC, Moon YK. Hormonal and nutritional regulation of lipogenic enzyme mRNA levels in rat primary white and brown adipocytes. *J Nutr Sci Vitaminol (tokyo)*. 2003;49:40–6. <https://doi.org/10.3177/JNSV.49.40>.
- Freake HC, Oppenheimer JH. Stimulation of S14 mRNA and lipogenesis in brown fat by hypothyroidism, cold exposure, and cafeteria feeding: evidence supporting a general role for S14 in lipogenesis and lipogenesis in the maintenance of thermogenesis. *Proc Natl Acad Sci U S A*. 1987;84:3070–4. <https://doi.org/10.1073/PNAS.84.9.3070>.
- Gautier L, Cope L, Bolstad BM, Irizarry RA. affy—analysis of Affymetrix GeneChip data at the probe level. *Bioinformatics*. 2004;20:307–15. <https://doi.org/10.1093/BIOINFORMATICS/BTG405>.
- Gondret F, Ferré P, Dugail I. ADD-1/SREBP-1 is a major determinant of tissue differential lipogenic capacity in mammalian and avian species. *J Lipid Res*. 2001;42:106.
- Green CD, Maceyka M, Cowart LA, Spiegel S. Sphingolipids in metabolic disease: the good, the bad, and the unknown. *Cell Metab*. 2021;33:1293–306. <https://doi.org/10.1016/J.CMET.2021.06.006>.
- Harper ME, Seifert EL. Thyroid hormone effects on mitochondrial energetics. *Thyroid*. 2008;18:145–56. <https://doi.org/10.1089/THY.2007.0250>.
- Haynes AS, Filippov V, Filippova M, Yang J, Zhang K, Duerksen-Hughes PJ. DNA damage induces down-regulation of UDP-glucose ceramide glucosyltransferase, increases ceramide levels and triggers apoptosis in p53-deficient cancer cells. *Biochim Biophys Acta*. 2012;1821:943. <https://doi.org/10.1016/J.BBALIP.2012.02.002>.
- Höring M, Ejsing CS, Hermansson M, Liebisch G. Quantification of cholesterol and cholesteryl ester by direct flow injection high-resolution fourier transform mass spectrometry utilizing species-specific response factors. *Anal Chem*. 2019;91:3459–66. <https://doi.org/10.1021/acs.analchem.8b05013>.
- Höring M, Ekroos K, Baker PRS, Connell L, Stadler SC, Burkhardt R, Liebisch G. Correction of isobaric overlap resulting from sodiated ions in lipidomics. *Anal Chem*. 2020;92:10966–70. <https://doi.org/10.1021/ACS.ANALCHEM.0C02408>.
- Höring M, Ejsing CS, Krautbauer S, Ertl VM, Burkhardt R, Liebisch G. Accurate quantification of lipid species affected by isobaric overlap in Fourier-transform mass spectrometry. *J Lipid Res*. 2021;62: 100050. <https://doi.org/10.1016/J.JLIR.2021.100050>.
- Huang PS, Chang CC, Wang CS, Lin KH. Functional roles of non-coding RNAs regulated by thyroid hormones in liver cancer. *Biomed J*. 2021;44:272–84. <https://doi.org/10.1016/J.BJ.2020.08.009>.
- Jiang H, Lei R, Ding SW, Zhu S. Skewer: a fast and accurate adapter trimmer for next-generation sequencing paired-end reads. *BMC Bioinform*. 2014;15:1–12. <https://doi.org/10.1186/1471-2105-15-182/FIGURES/5>.
- Jump DB. Rapid induction of rat liver S14 gene transcription by thyroid hormone. *J Biol Chem*. 1989;264:4698–703. [https://doi.org/10.1016/S0021-9258\(18\)83799-1](https://doi.org/10.1016/S0021-9258(18)83799-1).
- Jump DB, Narayan P, Towle H, Oppenheimer JH. Rapid effects of triiodothyronine on hepatic gene expression. Hybridization analysis of tissue-specific triiodothyronine regulation of mRNAs 14. *J Biol Chem*. 1984;259:2789–97. [https://doi.org/10.1016/S0021-9258\(17\)43215-7](https://doi.org/10.1016/S0021-9258(17)43215-7).
- Kajihara R, Numakawa T, Odaka H, Yaginuma Y, Fusaki N, Okumiya T, Furuya H, Inui S, Era T. Novel drug candidates improve ganglioside accumulation and neural dysfunction in GM1 gangliosidosis models with autophagy activation. *Stem Cell Reports*. 2020;14:909–23. <https://doi.org/10.1016/J.STEMCR.2020.03.012>.
- Kallio MA, Tuimala JT, Hupponen T, Klemelä P, Gentile M, Scheinin J, Koski M, Käksi J, Korpelainen EI. Chipster: user-friendly analysis software for microarray and other high-throughput data. *BMC Genomics*. 2011;12:1–14. <https://doi.org/10.1186/1471-2164-12-507/FIGURES/5>.
- Kim JB, Spiegelman BM. ADD1/SREBP1 promotes adipocyte differentiation and gene expression linked to fatty acid metabolism. *Genes Dev*. 1996;10:1096–107. <https://doi.org/10.1101/GAD.10.9.1096>.
- Kinlaw WB, Church JL, Harmon J, Mariash CN. Direct evidence for a role of the “spot 14” protein in the regulation of lipid synthesis. *J Biol Chem*. 1995;270:16615–8. <https://doi.org/10.1074/jbc.270.28.16615>.
- Knupp J, Martínez-Montañés F, Van Den Bergh F, Cottier S, Schneider R, Beard D, Chang A. Sphingolipid accumulation causes mitochondrial dysregulation and cell death. *Cell Death Differ*. 2017;24(24):2044–53. <https://doi.org/10.1038/cdd.2017.128>.
- LaFave LT, Augustin LB, Mariash CN. S14: insights from knockout mice. *Endocrinology*. 2006;147:4044–7. <https://doi.org/10.1210/EN.2006-0473>.
- Lanni A, Moreno M, Goglia F. Mitochondrial actions of thyroid hormone. *Compr Physiol*. 2016;6:1591–607. <https://doi.org/10.1002/CPHY.C150019>.
- Lee K, Um SH, Rhee DK, Pyo S. Interferon-alpha inhibits adipogenesis via regulation of JAK/STAT1 signaling. *Biochim Biophys Acta*. 2016;1860:2416–27. <https://doi.org/10.1016/J.BBAGEN.2016.07.009>.
- Leiria LO, Tseng YH. Lipidomics of brown and white adipose tissue: implications for energy metabolism. *Biochim Biophys Acta Mol Cell Biol Lipids*. 2020;1865:158788. <https://doi.org/10.1016/J.BBALIP.2020.158788>.
- Liebisch G, Drobnik W, Reil M, Trümbach B, Arnecke R, Olgemöller B, Roscher A, Schmitz G. Quantitative measurement of different ceramide species from crude cellular extracts by electrospray ionization tandem mass spectrometry (ESI-MS/MS). *J Lipid Res*. 1999;40:1539–46. [https://doi.org/10.1016/S0022-2275\(20\)33398-8](https://doi.org/10.1016/S0022-2275(20)33398-8).
- Liebisch G, Drobnik W, Lieser B, Schmitz G. High-throughput quantification of lysophosphatidylcholine by electrospray ionization tandem mass spectrometry. *Clin Chem*. 2002;48:2217–24. <https://doi.org/10.1093/CLINCHEM/48.12.2217>.
- Liebisch G, Lieser B, Rathenber J, Drobnik W, Schmitz G. High-throughput quantification of phosphatidylcholine and sphingomyelin by electrospray ionization tandem mass spectrometry coupled with isotope correction algorithm. *Biochim Biophys Acta Mol Cell Biol Lipids*. 2004;1686:108–17. <https://doi.org/10.1016/j.bbalip.2004.09.003>.
- Liebisch G, Fahy E, Aoki J, Dennis EA, Durand T, Ejsing CS, Fedorova M, Feussner I, Griffiths WJ, Köfeler H, Merrill AH, Murphy RC, O'Donnell VB, Oskolkova O, Subramaniam S, Wakelam MJO, Spener F. Update on LIPID MAPS classification, nomenclature, and shorthand notation for MS-derived lipid structures. *J Lipid Res*. 2020;61:1539–55. <https://doi.org/10.1194/JLR.S120001025>.
- Lipina C, Hundal HS. Ganglioside GM3 as a gatekeeper of obesity-associated insulin resistance: evidence and mechanisms. *FEBS Lett*. 2015;589:3221–7. <https://doi.org/10.1016/J.FEBSLET.2015.09.018>.
- Love MI, Huber W, Anders S. Moderated estimation of fold change and dispersion for RNA-seq data with DESeq2. *Genome Biol*. 2014;15:1–21. <https://doi.org/10.1186/S13059-014-0550-8/FIGURES/9>.
- Lowell BB, Shulman GI. Mitochondrial dysfunction and type 2 diabetes. *Science*. 2005;307:384–7. https://doi.org/10.1126/SCIENCE.1104343/ASSET/9AB92F2B-F27C-4F4B-9E2E-35D6928CC6FB/ASSETS/GRAPHIC/307_384_F2B.JPEG.
- Lynch L, Nowak M, Varghese B, Clark J, Hogan AE, Toxavidis V, Balk SP, O'Shea D, O'Farrelly C, Exley MA. Adipose tissue invariant NKT cells protect against diet-induced obesity and metabolic disorder through regulatory cytokine production. *Immunity*. 2012;37:574–87. <https://doi.org/10.1016/J.IMMUNI.2012.06.016>.

- Majeed Y, Halabi N, Madani AY, Engelke R, Bhagwat AM, Abdesselem H, Agha MV, Vakayil M, Courjaret R, Goswami N, Hamidane HB, Elrayess MA, Rafii A, Graumann J, Schmidt F, Mazloum NA. SIRT1 promotes lipid metabolism and mitochondrial biogenesis in adipocytes and coordinates adipogenesis by targeting key enzymatic pathways. *Sci Reports*. 2021;11(11):1–19. <https://doi.org/10.1038/s41598-021-87759-x>.
- Matyash V, Liebisch G, Kurzchalia TV, Shevchenko A, Schwudke D. Lipid extraction by methyl-tert-butyl ether for high-throughput lipidomics. *J Lipid Res*. 2008;49:1137. <https://doi.org/10.1194/JLR.D700041-JLR200>.
- McGillicuddy FC, Chiquoine EH, Hinkle CC, Kim RJ, Shah R, Roche HM, Smyth EM, Reilly MP. Interferon gamma attenuates insulin signaling, lipid storage, and differentiation in human adipocytes via activation of the JAK/STAT pathway. *J Biol Chem*. 2009;284:31936–44. <https://doi.org/10.1074/jbc.M109.061655>.
- Mizunoe Y, Kobayashi M, Tagawa R, Nakagawa Y, Shimano H, Higami Y. Association between lysosomal dysfunction and obesity-related pathology: a key knowledge to prevent metabolic syndrome. *Int J Mol Sci*. 2019. <https://doi.org/10.3390/IJMS20153688>.
- Monteith AJ, Kang S, Scott E, Hillman K, Rajfur Z, Jacobson K, Costello MJ, Vilen BJ. Defects in lysosomal maturation facilitate the activation of innate sensors in systemic lupus erythematosus. *Proc Natl Acad Sci U S A*. 2016;113:E2142–51. <https://doi.org/10.1073/PNAS.1513943113/-DCSUPPLEMENTAL>.
- Mysore R, Liebisch G, Zhou Y, Oikkonen VM, Nidhina Haridas PA. Angiopoietin-like 8 (Angptl8) controls adipocyte lipolysis and phospholipid composition. *Chem Phys Lipids*. 2017;207:246–52. <https://doi.org/10.1016/j.chemphyslip.2017.05.002>.
- Ortega FJ, Vazquez-Martin A, Moreno-Navarrete JM, Bassols J, Rodriguez-Hermosa J, Gironés J, Ricart W, Peral B, Tinahones FJ, Frühbeck G, Menendez JA, Fernandez-Real JM. Thyroid hormone responsive Spot 14 increases during differentiation of human adipocytes and its expression is down-regulated in obese subjects. *Int J Obes*. 2010;34:467–99. <https://doi.org/10.1038/ijo.2009.263>.
- Park J, Huh JY, Oh J, Kim JJ, Han SM, Shin KC, Jeon YG, Choe SS, Park J, Kim JB. Activation of invariant natural killer T cells stimulates adipose tissue remodeling via adipocyte death and birth in obesity. *Genes Dev*. 2019;33:1657–72. <https://doi.org/10.1101/GAD.329557.119>.
- Phipson B, Lee S, Majewski IJ, Alexander WS, Smyth GK. Robust hyperparameter estimation protects against hypervariable genes and improves power to detect differential expression. *Ann Appl Stat*. 2016;10:946. <https://doi.org/10.1214/16-AOAS920>.
- Pshezhetsky AV. Crosstalk between 2 organelles: lysosomal storage of heparan sulfate causes mitochondrial defects and neuronal death in mucopolysaccharidosis III type C. *Rare Dis (Austin, Tex)*. 2015;3:e1049793. <https://doi.org/10.1080/21675511.2015.1049793>.
- Raj K, Berman-Booty L, Foureman P, Giger U. ARSB gene variants causing Mucopolysaccharidosis VI in Miniature Pinscher and Miniature Schnauzer dogs. *Anim Genet*. 2020;51:982–6. <https://doi.org/10.1111/AGE.13005>.
- Rakhshandehroo M, van Eijkeren RJ, Gabriel TL, de Haar C, Gijzel SMW, Hamers N, Ferraz MJ, Aerts JMFG, Schipper HS, van Eijk M, Boes M, Kalkhoven E. Adipocytes harbor a glucosylceramide biosynthesis pathway involved in iNKT cell activation. *Biochim. Biophys Acta Mol Cell Biol Lipids*. 2019;1864:1157–67. <https://doi.org/10.1016/j.bbalip.2019.04.016>.
- Rocha M, Apostolova N, Diaz-Rua R, Muntane J, Victor VM. Mitochondria and T2D: role of autophagy, ER stress, and inflammasome. *Trends Endocrinol Metab*. 2020. <https://doi.org/10.1016/j.tem.2020.03.004>.
- Roszczyk-Owsiejczuk K, Zabielski P. Sphingolipids as a culprit of mitochondrial dysfunction in insulin resistance and type 2 diabetes. *Front Endocrinol (Lausanne)*. 2021;12:143. <https://doi.org/10.3389/FENDO.2021.635175/BIBTEX>.
- Ryysy L, Häkkinen AM, Goto T, Vehkavaara S, Westerbacka J, Halavaara J, Yki-Järvinen H. Hepatic fat content and insulin action on free fatty acids and glucose metabolism rather than insulin absorption are associated with insulin requirements during insulin therapy in type 2 diabetic patients. *Diabetes*. 2000;49:749–58. <https://doi.org/10.2337/DIABETES.49.5.749>.
- Sasaki N, Itakura Y, Toyoda M. Ganglioside GM1 contributes to extracellular/intracellular regulation of insulin resistance, impairment of insulin signaling and down-stream eNOS activation, in human aortic endothelial cells after short- or long-term exposure to TNF α . *Oncotarget*. 2018;9:5562. <https://doi.org/10.18632/ONCOTARGET.23726>.
- Sayre NL, Lechleiter JD. Fatty acid metabolism and thyroid hormones. *Curr Trends Endocrinol*. 2012;6:65.
- Schömel N, Gruber L, Alexopoulos SJ, Trautmann S, Olzomer EM, Byrne FL, Hoehn KL, Gurke R, Thomas D, Ferreirós N, Geisslinger G, Wegner MS. UGCG overexpression leads to increased glycolysis and increased oxidative phosphorylation of breast cancer cells. *Sci Rep*. 2020;10(10):1–13. <https://doi.org/10.1038/s41598-020-65182-y>.
- Schöttl T, Kappler L, Fromme T, Klingenspor M. Limited OXPHOS capacity in white adipocytes is a hallmark of obesity in laboratory mice irrespective of the glucose tolerance status. *Mol Metab*. 2015;4:631–42. <https://doi.org/10.1016/J.MOLMET.2015.07.001>.
- Seelig S, Liaw C, Towle HC, Oppenheimer JH. Thyroid hormone attenuates and augments hepatic gene expression at a pretranslational level. *Proc Natl Acad Sci U S A*. 1981;78:4733. <https://doi.org/10.1073/PNAS.78.8.4733>.
- Simonis H, Yaghootfam C, Sylvester M, Gieselmann V, Matzner U. Evolutionary redesign of the lysosomal enzyme arylsulfatase A increases efficacy of enzyme replacement therapy for metachromatic leukodystrophy. *Hum Mol Genet*. 2019;28:1810–21. <https://doi.org/10.1093/HMG/DDZ020>.
- Sinha RA, Singh BK, Yen PM. Direct effects of thyroid hormones on hepatic lipid metabolism. *Nat Rev Endocrinol*. 2018;14:259. <https://doi.org/10.1038/NREND0.2018.10>.
- Soronen J, Laurila PP, Naukkarinen J, Surakka I, Ripatti S, Jauhainen M, Oikkonen VM, Yki-Järvinen H. Adipose tissue gene expression analysis reveals changes in inflammatory, mitochondrial respiratory and lipid metabolic pathways in obese insulin-resistant subjects. *BMC Med Genomics*. 2012;5:9. <https://doi.org/10.1186/1755-8794-5-9>.
- Tomanin R, Karageorgos L, Zanetti A, Al-Sayed M, Bailey M, Miller N, Sakuraba H, Hopwood JJ. Mucopolysaccharidosis type VI (MPS VI) and molecular analysis: review and classification of published variants in the ARSB gene. *Hum Mutat*. 2018;39:1788–802. <https://doi.org/10.1002/HUMU.23613>.
- Trabszo C, Ramms B, Chopra P, Lüllmann-Rauch R, Stroobants S, Sproß J, Jeschke A, Schinke T, Boons GJ, Esko JD, Lübke T, Dieks T. Arylsulfatase K inactivation causes mucopolysaccharidosis due to deficient glucuronate desulfation of heparan and chondroitin sulfate. *Biochem J*. 2020;477:3433–51. <https://doi.org/10.1042/BCJ20200546>.
- van Eijkeren RJ, Krabbe O, Boes M, Schipper HS, Kalkhoven E. Endogenous lipid antigens for invariant natural killer T cells hold the reins in adipose tissue homeostasis. *Immunology*. 2018;153:179. <https://doi.org/10.1111/IMM.12839>.
- van Eijkeren RJ, Morris J, Borgman A, Markovska A, Kalkhoven E. Cytokine output of adipocyte-iNKT cell interplay is skewed by a lipid-rich micro-environment. *Front Endocrinol (Lausanne)*. 2020. <https://doi.org/10.3389/FENDO.2020.00479/FULL>.
- Van Der Kolk BW, Muniandy M, Kaminska D, Alvarez M, Ko A, Miao Z, Valsesia A, Langin D, Vaittinen M, Pääkkönen M, Jokinen R, Kaye S, Heinonen S, Virtanen KA, Andersson DP, Männistö V, Saris WH, Astrup A, Rydén M, Blak EE, Pajukanta P, Pihlajamäki J, Pietiläinen KH. Differential mitochondrial gene expression in adipose tissue following weight loss induced by diet or bariatric surgery. *J Clin Endocrinol Metab*. 2021;106:1312–24. <https://doi.org/10.1210/CLINEM/DGAB072>.
- Vernochet C, Damilano F, Mourier A, Bezy O, Mori MA, Smyth G, Rosenzweig A, Larsson NG, Kahn CR. Adipose tissue mitochondrial dysfunction triggers a lipodystrophic syndrome with insulin resistance, hepatosteatosis, and cardiovascular complications. *FASEB J*. 2014;28:4408–19. <https://doi.org/10.1096/FJ.14-253971>.
- Wabitsch M, Brenner RE, Melzner I, Braun M, Möller P, Heinze E, Debatin KM, Hauner H. Characterization of a human preadipocyte cell strain with high capacity for adipose differentiation. *Int J Obes Relat Metab Disord*. 2001;25:8–15. <https://doi.org/10.1038/SJJO.0801520>.
- Wang X, Carre W, Zhou H, Lamont SJ, Cogburn LA. Duplicated Spot 14 genes in the chicken: Characterization and identification of polymorphisms associated with abdominal fat traits. *Gene*. 2004;332:79–88. <https://doi.org/10.1016/j.gene.2004.02.021>.
- Wang HB, Li H, Wang QG, Zhang XY, Wang SZ, Wang YX, Wang XP. Profiling of chicken adipose tissue gene expression by genome array. *BMC Genomics*. 2007. <https://doi.org/10.1186/1471-2164-8-193>.
- Wang Q, Zou J, Zhang X, Mu H, Yin Y, Xie P. Glucosylceramide synthase promotes Bcl-2 expression via the ERK signaling pathway in the K562/A02 leukemia drug-resistant cell line. *Int J Hematol*. 2014;100:559–66. <https://doi.org/10.1007/S12185-014-1679-7>.

- Weitzel JM, Iwen KAH, Seitz HJ. Regulation of mitochondrial biogenesis by thyroid hormone. *Exp Physiol*. 2003;88:121–8. <https://doi.org/10.1113/EPH8802506>.
- Wensveen FM, Jelenčić V, Valentić S, Šestan M, Wensveen TT, Theurich S, Glasner A, Mendrila D, Štimac D, Wunderlich FT, Brüning JC, Mandelboim O, Polić B. NK cells link obesity-induced adipose stress to inflammation and insulin resistance. *Nat Immunol*. 2015;16:376–85. <https://doi.org/10.1038/NI.3120>.
- Westerbacka J, Cornér A, Kannisto K, Kolak M, Makkonen J, Korshennikova E, Nyman T, Hamsten A, Fisher RM, Yki-Järvinen H. Acute in vivo effects of insulin on gene expression in adipose tissue in insulin-resistant and insulin-sensitive subjects. *Diabetologia*. 2006;49:132–40. <https://doi.org/10.1007/S00125-005-0075-5/FIGURES/3>.
- Wieser V, Adolph TE, Grander C, Grabherr F, Enrich B, Moser P, Moschen AR, Kaser S, Tilg H. Adipose type I interferon signalling protects against metabolic dysfunction. *Gut*. 2018;67:157–65. <https://doi.org/10.1136/GUTJNL-2016-313155>.
- Woerle HJ, Meyer C, Dostou JM, Gosmanov NR, Islam N, Popa E, Wittlin SD, Welle SL, Gerich JE. Pathways for glucose disposal after meal ingestion in humans. *Am J Physiol Endocrinol Metab*. 2003. <https://doi.org/10.1152/AJPENDO.00365.2002/ASSET/IMAGES/LARGE/H10431209006.JPEG>.
- Woo CY, Jang JE, Lee SE, Koh EH, Lee KU. Mitochondrial dysfunction in adipocytes as a primary cause of adipose tissue inflammation. *Diabetes Metab J*. 2019;43:247. <https://doi.org/10.4093/DMJ.2018.0221>.
- Wu J, Wang C, Li S, Li S, Wang W, Li J, Chi Y, Yang H, Kong X, Zhou Y, Dong C, Wang F, Xu G, Yang J, Gustafsson J-Å, Guan Y. Thyroid hormone-responsive SPOT 14 homolog promotes hepatic lipogenesis, and its expression is regulated by Liver X receptor α through a sterol regulatory element-binding protein 1c-dependent mechanism in mice. *Hepatology*. 2013;58:617–28. <https://doi.org/10.1002/HEP26272>.
- Yamashita T, Hashiramoto A, Haluzik M, Mizukami H, Beck S, Norton A, Kono M, Tsuji S, Daniotti JL, Werth N, Sandhoff R, Sandhoff K, Proia RL. Enhanced insulin sensitivity in mice lacking ganglioside GM3. *Proc Natl Acad Sci*. 2003;100:3445–9. <https://doi.org/10.1073/PNAS.0635898100>.
- Yki-Järvinen H, DeFronzo RA, Koivisto VA. Normalization of insulin sensitivity in type I diabetic subjects by physical training during insulin pump therapy. *Diabetes Care*. 1984;7:520–7. <https://doi.org/10.2337/DIACARE.7.6.520>.
- Yu G, He QY. ReactomePA: an R/Bioconductor package for reactome pathway analysis and visualization. *Mol Biosyst*. 2016;12:477–9. <https://doi.org/10.1039/C5MB00663E>.
- Zemski Berry KA, Murphy RC. Electrospray ionization tandem mass spectrometry of glycerophosphoethanolamine plasmalogen phospholipids. *J Am Soc Mass Spectrom*. 2004;15:1499–508. <https://doi.org/10.1016/J.JASMS.2004.07.009>.
- Zhu Q, Mariash A, Margosian MR, Gopinath S, Fareed MT, Anderson GW, Mariash CN. Spot 14 gene deletion increases hepatic de novo lipogenesis. *Endocrinology*. 2001;142:4363–70. <https://doi.org/10.1210/ENDO.142.10.8431>.

Publisher's Note

Springer Nature remains neutral with regard to jurisdictional claims in published maps and institutional affiliations.

Ready to submit your research? Choose BMC and benefit from:

- fast, convenient online submission
- thorough peer review by experienced researchers in your field
- rapid publication on acceptance
- support for research data, including large and complex data types
- gold Open Access which fosters wider collaboration and increased citations
- maximum visibility for your research: over 100M website views per year

At BMC, research is always in progress.

Learn more biomedcentral.com/submissions

